Preparation and Characterization of Carboxymethyl Konjac Glucomannan/Sodium Montmorillonite Hybrid Films

Jun Lu, Chaobo Xiao

College of Chemistry and Molecular Sciences, Wuhan University, Wuhan, Hubei 430072, People's Republic of China

Received 12 January 2006; accepted 16 July 2006
DOI 10.1002/app.25440
Published online in Wiley InterScience (www.interscience.wiley.com).

ABSTRACT: Carboxymethyl konjac glucomannan (CKGM)/sodium montmorillonite (MMT) hybrid films of various compositions were prepared by casting from a polymer/silicate water suspension. The structure and properties of the hybrid films were investigated by wide angle X-ray diffraction (WAXD), transmission electron microscopy (TEM), attenuated total reflection infrared spectroscopy (ATR-IR), differential scanning calorimetry (DSC), and tensile tests. The results from WXRD and TEM indicated that an intercalated CKGM/MMT nanocomposite film was obtained by polymer solution intercalation. WXRD and DSC showed that the high-T_m crystal phase was induced by the presence of lower MMT loading, but the T_m of the hybrid films became weak with the increase of MMT content due to the polymer confinement. The hybrid films showed higher thermal stability and mechanical properties than that of the neat polysaccharide due to the strong interaction between hydroxyl and carbonyl group of CKGM and the silicate layer of MMT. Furthermore, the degree of swelling of the hybrid films was investigated in acidic buffer solutions. © 2006 Wiley Periodicals, Inc. J Appl Polym Sci 103: 2954–2961, 2007

Key words: carboxymethyl konjac glucomannan; clay; intercalation

INTRODUCTION

There is an ever-increasing interest in the utilization of renewable materials. Among natural polymers, Konjac glucomannan (KGM) has attracted great interests since it exhibits expected properties, such as easily modification, high viscosity, and excellent film-forming ability besides availability, low cost, good biocompatibility, and biodegradability. KGM, one of the high molecular weight water-soluble nonionic natural polysaccharide found in tubers of the *Amorphophallus konjac*, is composed of β-(1→4)linked D-glucose and D-mannose in the molar ratio of 1 : 1.6 with a low degree of acetyl groups[1] and it forms highly viscous solutions when dissolved in water.[2] KGM has been used in the fields of food, pharmaceuticals, and chemical engineering. However, the use of KGM as a material is limited by its poor stability and processing. Therefore, chemical and physical modification has been applied to improve these properties, in addition to provide the functional properties of polysaccharides. It is noted that carboxymethyl konjac glucomannan (CKGM) has significant enhancements of water solubility, stability, functions[3] and new applications in industrial[4] and biomedical fields[5,6] compared to the unmodified KGM. But it is known that the improvements are at the cost of mechanical properties of materials. Consequently, it is usually blended with hydrophobic biodegradable polymers[7,8] or crosslinked by organic reagents to improve the material's mechanical properties.

A novel method for improving polysaccharide properties is adding clay to polysaccharide formulations. In recent years, a little polysaccharide/clay nanocomposites with greatly improved barrier, mechanical and heat resistance properties have been reported, such as thermoplastic starch,[9,10] cellulose,[11] gelatin,[12] and chitosan.[13] However, little research on KGM or its derivatives and clay hybrids has been carried out. It is well known that sodium montmorillonite (MMT) is a naturally occurring 2 : 1 phyllosilicate, capable of forming stable suspensions in water. This hydrophilic character of MMT also promotes dispersion of these inorganic crystalline layers in water-soluble polymers.[14,15] Moreover, MMT has excellent exchanged cations capability and reactive OH groups at the surface.[16] Inspired from those studies, this work is focused on investigating the properties of CKGM/MMT hybrid films.

In the present investigation, CKGM was synthesized and CKGM/MMT hybrid films of various compositions were obtained. The dispersion of MMT into the CKGM matrix and the effect of its addition on the mechanical, thermal properties, morphology, and interaction of CKGM/MMT hybrids were studied.

Correspondence to: C. Xiao (cbxiao@whu.edu.cn).
Contract grant sponsor: Education Office of Hubei Province, People's Republic of China; contract grant numbers: D200525003 and D200625004.

Journal of Applied Polymer Science, Vol. 103, 2954–2961 (2007)

We predict that this work may contribute basic information to the further application of KGM and its erivatives in packaging films and biomedical materials.

EXPERIMENTAL

Materials

KGM powder (purity 99%) was purchased from Huaxianzi Konjac (Hubei, China) and was used without further purification. The viscosity is 10 Pa s in 1 wt % concentration.

The preparation of CKGM was as follows.[17] KGM (4 g) was soaked in 8 mL of 50 wt % aqueous methanol. After 1 h, the swollen KGM was suspended in 20 mL of methanol and 8 mL of 30 wt % aqueous solution of sodium hydroxide was added gradually while stirring at 50°C. After 1.5 h, 3 g of monochloroacetic acid (MCA) was then added gradually. Mechanical stirring was continued for 40 h at 50°C. At this point, the mixture was neutralized with 30 wt % hydrochloric acid to a pH of 6. The product was washed with 70, 80, and 100 wt % methanol to remove impurities, successively, and filtered off. The residue was dried at 50°C in vacuum to obtain the pure CKGM.

Sodium MMT (the particle size is 33 μm) was supplied by Zhejiang Fenghong Clay Chemicals (Zhejiang, China). Other reagents were all of analytical grade.

Preparation of CKGM/MMT composite films

Hybrids were synthesized by a solution-intercalation film-casting method. The CKGM/MMT ratios were 100/0, 95/05, 90/10, 85/15, 80/20, 70/30, and 50/50 (W/W), relative to dry CKGM, with a total mass of 1.0 g. MMT was dispersed in distilled water to form a suspension of MMT at a concentration of 2 wt %. The suspension was stirred for 24 h. CKGM was dissolved in distilled water and was added to the stirring suspensions. The mixtures were stirred vigorously at 60°C for 48 h and degassed, and then were poured on to glass plates and water evaporated at room temperature for 3 days. The films of different ratios above were coded as CM0, CM5, CM10, CM15, CM20, CM30, CM50, respectively.

X-ray diffraction

Wide-angle X-ray diffraction (WAXD) patterns were recorded on an X-ray diffraction instrument (XRD-6000 Shimadzu, Japan), by using CuKå radiation ($\lambda = 0.1542$ nm) at 40 kV and 30 mA with a scan rate of 4° min^{-1}. The diffraction angle ranged from 2° to 45°.

Transmission electron microscopy

TEM was performed in a Hitachi HF-2000, which used a high-vacuum cold cathode field emission gun as the electron source. A piece of the film was placed in epoxy resin and later microtomed into 200 nm slices, which were placed upon nickel TEM grids.

ATR-IR spectroscopy

IR spectra of the films were recorded using a Fourier transform infrared (FTIR) spectrometer (Nicolet 170SX) with attenuated total reflection instruments for investigation intermolecular interaction. The films were taken on the flat sheet and data were collected over 64 scans with a resolution of 4 cm^{-1} at room temperature.

Differential scanning calorimetry

DSC was performed using a Netzsch DSC 200 PC at a heating rate of 20°C/min under nitrogen atmosphere. The temperature ranged from 45 to 500°C.

Thermogravimetry analysis

Thermal gravimetric measurements were performed using Netzsch STA 449C instrument (Germany) under a nitrogen atmosphere with a flow capacity of 30 mL/min. The scan was carried out at a heating rate of 10°C/min from 40 to 800°C. The sample weight was about 8–10 mg and analyzed using α-Al_2O_3 crucible.

Tensile tests

Tensile strength and elongation at break of the films were measured on a versatile electron tensile tester (CMT-6503, Shenzhen SANS Test Machine, China) with a tensile rate of 5 mm/min. The size of the films strips was 70 × 10 × 50 mm^3 (length × width × distance between two clamps).

Swelling study

The degree of swelling (Q_w) of CKGM and hybrid films were measured by the following

$$Q_w = (W_{wet} - W_{dry})/W_{dry}$$

Where W_{wet} is the weight of wet films and W_{dry} is the weight of dried films. The experimental process was performed as follows: 0.1 g films were immersed in 200 mL hexamethylene tetramine/hydrochloric acid buffer solution with various pH values for 24 h to reach swelling equilibrium. The swollen films were taken out and weighed after the excess of water lying on the surfaces was absorbed with a filter paper. Then calculate according to the formulas above.

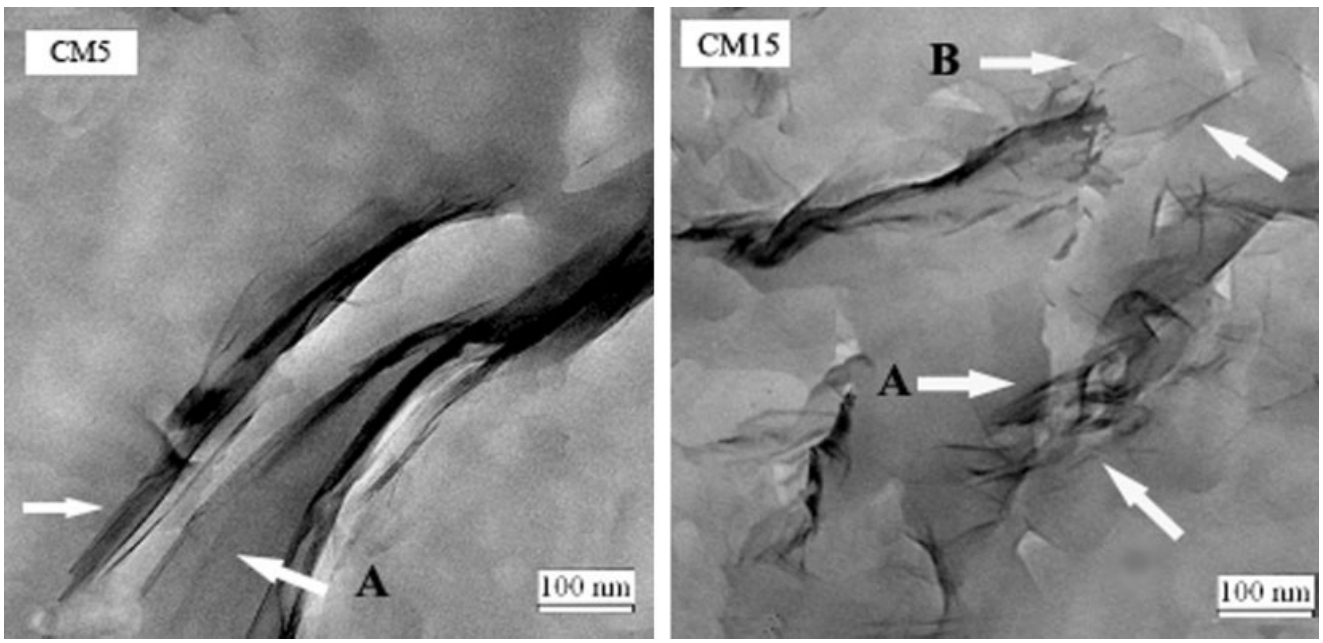

Figure 1 TEM images of the hybrid films of CM5 and CM15. The intercalation is labeled (A), Exfoliation is labeled (B).

RESULTS AND DISCUSSION

Dispersion of inorganic layers

With the emphasis on the dispersion of the nanometer-thin layered fillers in the polymer matrix, TEM was used to directly view the hybrid structure for nanocomposites. Figure 1 shows the TEM images for the different CKGM-MMT ratio hybrid films. The dark lines in the pictures represent clay layers, the spaces between the dark lines are interlayer spaces, and the gray bases represent CKGM matrix. In the image of CM5, most silicate layers existed as tactoids; however, in some parts, intercalation (label ''A'') was seen a little. In the image of CM15, there were still some tactoids, and exfoliation (label ''B'') was observed a little; however, in some parts, silicate layers were separated by ultrathin CKGM, and intercalation was seen clearly. This indicates that clay dispersion in CKGM was mainly in the intercalated state and depended on the CKGM/MMT weight ratio.

The periodic intercalated structure was quantified through WXRD. Figure 2 shows the XRD patterns of CM0, CM5, CM10, CM15, CM20, CM30, CM50, and MMT. The intercalation of CKGM in the clay interlayer was confirmed by the decrease of 2θ values while the CKGM-MMT ratio increased. MMT had a sharp peak at $2\theta = 7.1^\circ$, corresponding to a basal spacing of 1.25 nm. All diffraction peaks of hybrids shifted toward lower angle values and became broad. It can be seen that the interlayer spacing increased from 1.25 nm for MMT to 2.63 nm for CM15. However, the diffraction peak of hybrids shifted to higher angle values when the MMT content was over 15 wt % and the corresponding basal spacing decreased from 2.63 nm for CM15 to 1.67 nm for CM50.

Interestingly, clay dispersion in CM15 was better than that of CM5 from the TEM images and XRD patterns of the hybrids. It seems to be at odds with the theoretical expectations. In our case, we found that the hybrid structure was actually kinetically dictated rather than thermodynamics when the MMT content was lower to 5 wt %. In the water solution of CKGM and MMT, the layers remained in colloidal suspension. When a few CKGM chains intercalated into the MMT layer, crystal behavior was induced soon and crystal phase of CKGM appeared, the chain mobility of CKGM decreased and no further intercalation occurred. In a word, the crystal phase was induced by the presence of the silicate layers.[18] With the increase of MMT content, most CKGM chains entered into the MMT layer, crystals were constrained. This result was confirmed by the XRD patterns of the hybrids in Figure 3. In the 2θ region between 10° and 25°, CKGM had its crystalline reflections corresponding to $2\theta = 12.7^\circ$, 18.7°, 21.9°, respectively. In the same region, MMT also had its reflection at 21.9°. The crystalline peaks of CM5 were higher apparently in intensity than that of pure CKGM. With the increase of MMT content, the intensity became lower. In addition, DSC provided evidence that lower loading of MMT should promote polymer crystal. We should discuss it later.

ATR-IR analysis

We explored the interaction between CKGM and MMT by ATR-IR. Figure 4 shows the ATR-IR spectra

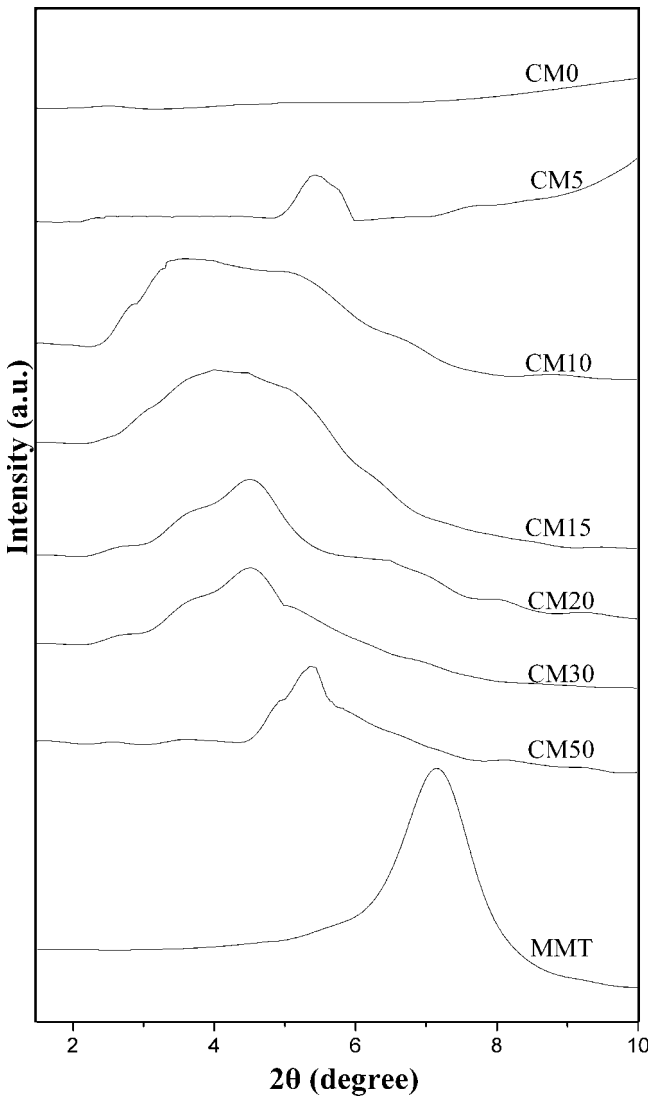

Figure 2 WXRD patterns of MMT and the hybrid films.

of CM0, CM5, CM10, CM15, and MMT in the 4000–500 cm^{-1} wave number range. It is noted that the stretching of carbonyl at 1658 cm^{-1} of CKGM.[19] disappeared and the stretching vibration of ether bond at 1028 cm^{-1} of CKGM shifted to a lower wave number with the increase of MMT content, which is attributed to the formation of new hydrogen bonds between —C=O, —O in CKGM and —OH in the silicate layer of MMT. The vibration band characteristics of the silicate, the deformation vibration of hydroxyl at 1640 cm^{-1} was disappeared in the hybrid films; the stretching vibration of Si—O at 1042 cm^{-1} overlapping with the band of ether in CKGM shifted to the lower wave number, indicating that the interaction between —OH, Si—O in MMT, and —OH in CKGM occurred, according to the study of Hwan-Man et al.[20] Some main bands for distinctive functional groups were identical in pure CKGM and pure MMT, which makes observation of any modification in these bands difficult. However, intensity changes in the modes below 800 cm^{-1} were observed, more specifically at 807 and 876 cm^{-1}, these bands were due to skeletal modes, low frequency vibrations of the ring.[21] The intensity of these bands decreased with the increase of MMT content reaching a constant value at a clay content of over 15 wt %. These results showed that vibration of the glucose ring was affected by the presence of clay possibly due to conformational changes. Therefore, it was due to the strong interaction between hydroxyl and carbonyl group of CKGM and the silicate layer of MMT that the intercalation occurred.

Thermal analysis

Thermal properties were investigated from DSC curves recorded in the 45–500°C range. As Figure 5 showed, pure CKGM had T_m peak at 125°C. The T_m peak of CM5 became stronger and shifted to 162.5°C. This clearly suggested that the high-T_m crystal phase was induced by the presence of lower MMT loading.

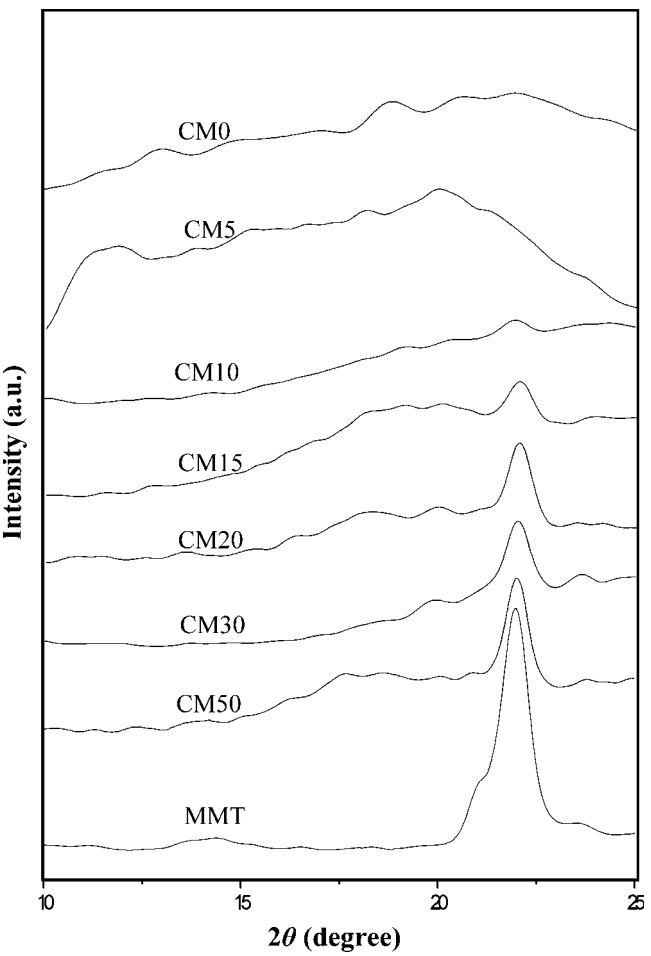

Figure 3 WXRD of the crystal peaks of the hybrids and MMT.

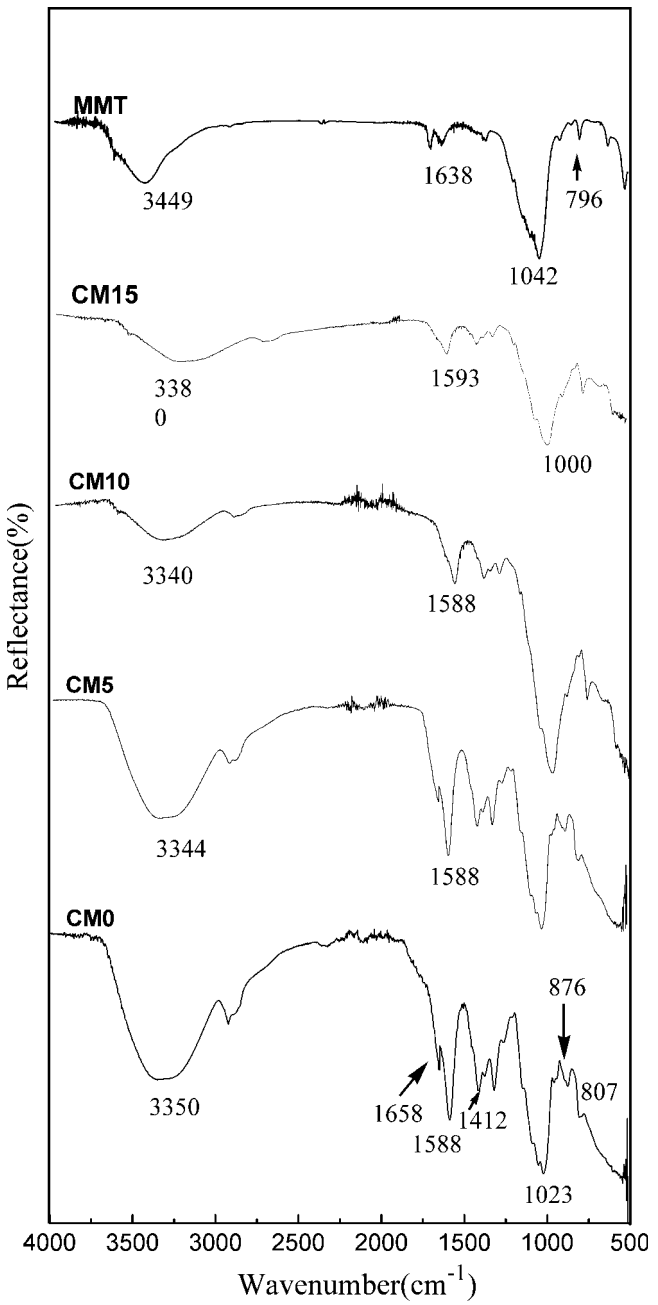

Figure 4 IR spectra of MMT and the hybrid films.

With the increase of MMT content, the T_m peak became weak and broad, shifted to around 90°C. This result may be explained that CKGM chains which intercalated into the interlayer of MMT were restricted by sheets of MMT, and the movement of segments was restrained. In addition, there existed polar interaction or hydrogen bond between functional groups of CKGM chains and the sheets of MMT; MMT also acted as physical crosslinking sites, and reduced the activity of CKGM matrix. Therefore, the T_m peaks became weak and broad.

In the range of 200–400°C, all the hybrid films showed distinct dual exothermic peaks compared to the overlapping peaks of pure CKGM, the first one was attributed to the breaking of intermolecular hydrogen bonds and the higher one was attributed to the breaking of intramolecular hydrogen bonds and the molecular side chains. It can be seen that the degradation temperature of the hybrid films increased gradually with the increase of the MMT content, and became level off when the MMT content was beyond 15 wt %. The first thermal degradation temperature of CM15 (299°C) was 14°C higher than that of pure CKGM (285°C). Therefore, CM15 had relatively high thermal stability.

TGA was used to investigate the thermal degradation patterns of the films. As shown in Figure 6, the TG curves of pure CKGM showed two degradation steps attributable to water loss and to CKGM degradation; pure clay showed a small weight loss about 9.1 wt % in the range of 50–100°C attributable to water loss and remained unchanged when heated to 500°C due to its thermally resistance.[22] The hybrid films showed two degradation steps attributable to the breaking of intermolecular hydrogen bonds, the breaking of intramolecular hydrogen bonds and the molecular side chains in the range from 200 to 630°C. Compared to pure CKGM, the thermal stability of the films was shown in Table I. The hybrid films showed higher beginning disintegration temperature at 250°C for CM15 and less weight loss (57 wt %) than that of

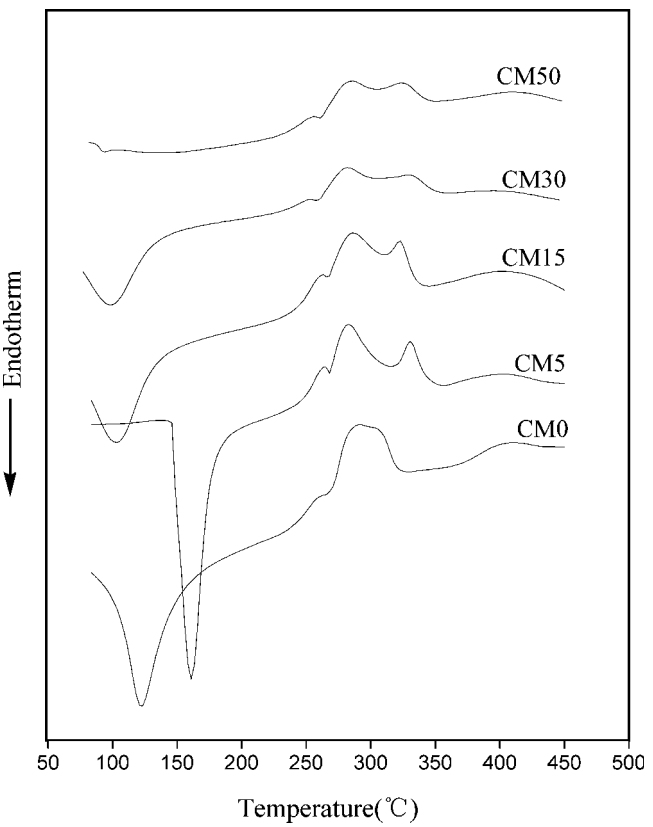

Figure 5 DSC curves of the hybrid films.

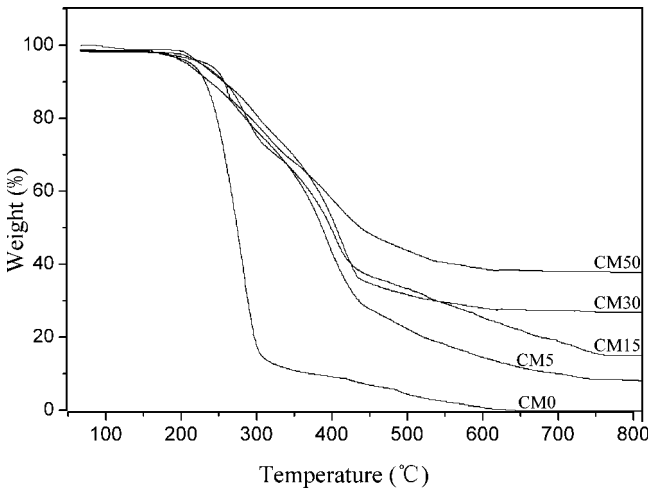

Figure 6 TG curves of the hybrid films.

pure CKGM (210°C, 78 wt %), suggesting an enhancement of thermal stability for the hybrid films. After approximately 650°C, the curves all became flat, and mainly the inorganic residues remained. It also can be seen that the hybrid films displayed a residue proportional to its clay content.

The improvement on thermal stability of the hybrids is mainly attributed to two aspects. The first aspect, it was due to thermal resistance of MMT and the nanodispersion of MMT layers in the CKGM matrix. Nanoscale MMT layers had an excellent barrier property in preventing the release of degraded CKGM fragments. The second aspect was that there was strong hydrogen bonds interaction between MMT and CKGM in the hybrids, and MMT acted as physical crosslinking sites to retard the thermal decomposition of CKGM to a certain extent. So intercalation with MMT is helpful to improve thermal stability of CKGM.

Mechanical properties

The effect of the MMT content on the mechanical properties of the hybrid films was illustrated in Figure 7. The Young's modulus (E'), stress-at-break (σ_b) and strain-at-break (ε_b) of pure KGM were 3.5 GPa, 58.1 MPa, and 4.4% while that of pure CKGM were lower to 2.0 GPa, 39.5 MPa, and 4.8%. As shown in Figure 7, it suggested that intercalation with MMT can improve the mechanical properties of CKGM. With the increase of the MMT content, the tensile strength and Young's modulus of the hybrids were enhanced and the maximum values were observed at 15 wt % MMT content. This behavior can be explained by the fact that MMT layers had dispersed in nanoscale in CKGM matrix and had huge surface area exposed to polymer, then the polymer matrix

TABLE I
Thermal Stability of the Films

Sample	Onset temperature (°C)	End temperature (°C)	Weight loss (%)
CM0	210	330	78
CM5	240	460	69
CM15	250	450	57
CM30	240	440	65
CM50	240	450	48

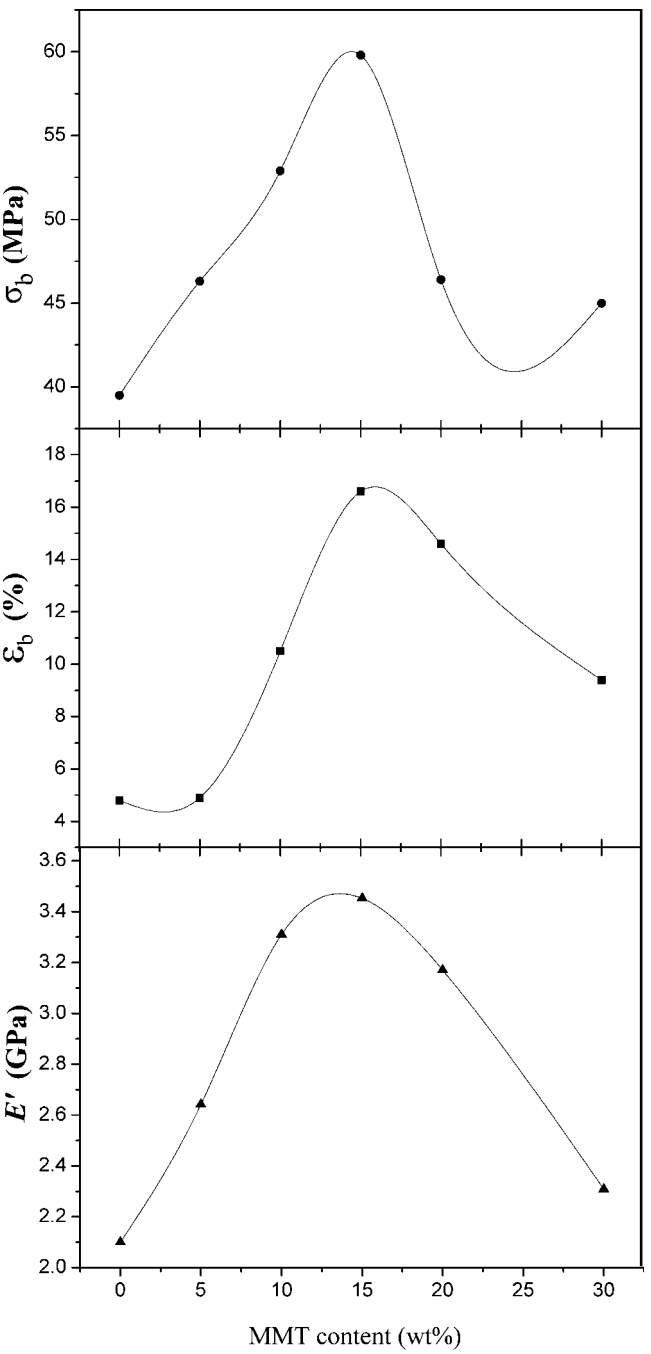

Figure 7 Mechanical properties as a function of the MMT content.

was physisorbed on the silicate surfaces and was stiffened through its affinity.[23] In addition, the strong interaction between the polysaccharide and the silicate surfaces became strength. As the MMT content was over 15%, the tensile strength and Young's modulus began to decrease, which may arise from the aggregation of MMT particles with higher surface energy when the MMT content was high enough.

Compared to pure CKGM, the hybrids displayed higher strain-at-break values with the increase of MMT content and reached 16.6% strain-at-break at 15 wt % MMT content. It indicated that the proper intercalation of CKGM into MMT improved the strain-at-break of the films. However, the strain-at-break values decreased when MMT content over 15 wt %. This indicated that adding the inorganic filler into a polymeric matrix increased its brittleness when beyond the limit.[24]

Swelling tests

Owing to our interest in developing polymeric materials with improved properties, we have studied the degree of swelling of the hybrid films in acidic buffer solutions.

As a polyelectrolyte, the ionized states of CKGM are dependent on pH. It is well known that uncrosslinked CKGM is easily dissolved in basic solution while swells in acidic solution. As shown in Figure 8, the degree of swelling of the hybrid films in pH 7 solution were higher than that of pure CKGM' and the maximum value was observed at 15 wt % MMT content. In the hybrid films, the silicate layers intercalated with polymeric matrix acted as physical crosslinking sites and a networks-like structure formed.[16]

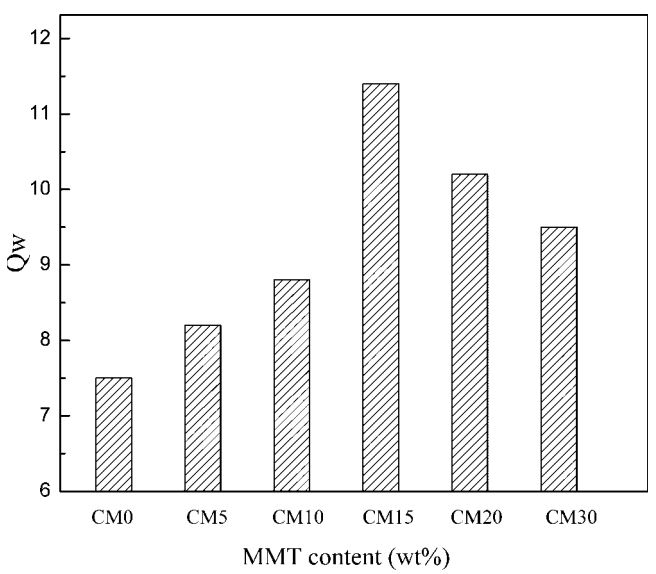

Figure 8 Variation of Q_w with the MMT content in the films.

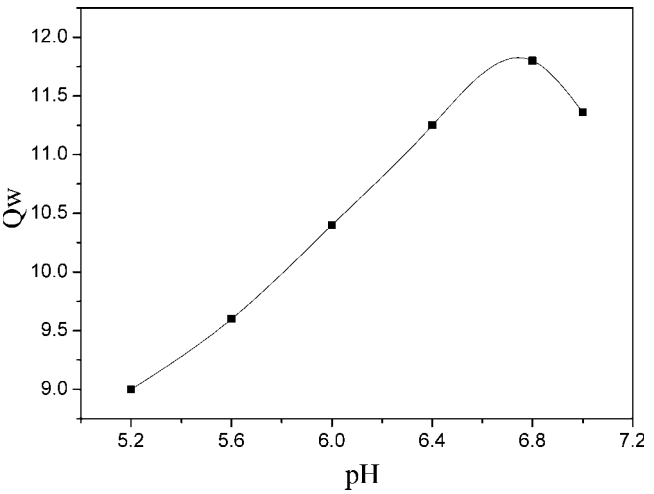

Figure 9 Variation of Q_w with pH for the film CM15.

Therefore, the water absorption of the films increased with the adding of MMT. But with larger amounts of MMT (beyond 15%), MMT aggregated and the place between crosslinking points decreased, then the water absorption of the films decreased.

The degree of swelling of the film CM15 depended on pH are shown in Figure 9. In the range of pH 5–pH 7, the maximum value of Q_w was observed at pH 6.8. It can be explained that CKGM belongs to a polyelectrolyte, it shows an extended structure in higher pH, which may facilitate the intercalation; it shows coiled structure in lower pH solution, which may destroy the intercalation of the polymer.[25] Moreover, the surface charges of MMT layer were changed with various pH[26] and the physical crosslinking sites were decreased. Therefore, Q_w increased with the increasing of pH. Regrettably, the films decomposed in 2 h in the range of below pH 5 or beyond pH 7.2. These results implied that the hybrid films had considerable water storing ability and potential use in biomaterial field.

CONCLUSIONS

CKGM/MMT hybrid films of various compositions were prepared by casting from a polymer/silicate water suspension. The structure characterization by WAXD, TEM ATR-IR of the hybrid films suggested that an intercalated CKGM/MMT nanocomposite film was obtained by polymer solution intercalation. WXRD and DSC showed that the high-T_m crystal phase was induced by the presence of lower MMT loading, but the T_m of the hybrid films became weak with the increase of MMT content, which due to the polymer confinement. The hybrid films showed higher thermal stability and mechanical properties than that of pure CKGM due to the strong interaction between hydroxyl and carbonyl group of CKGM and

the silicate layer of MMT, which can be confirmed by ATR-IR. Furthermore, the degree of swelling of the hybrid films became higher than that of pure CKGM in weak acidic solution. The results suggested that the hybrid films of CKGM/MMT had potential application for water storage materials with good thermal and mechanical properties.

References

1. Maeda, M.; Shimahara, H.; Sugiyama, N. Agric Biol Chem 1980, 38, 315.
2. Tye, R. J. Food Technol 1991, 45, 82.
3. Kobayashi, S.; Tsujihata, S.; Hibi, N. Food Hydrocolloids 2002, 16, 289.
4. Feng, C. G.; Luo, L. X. Ion Exch Adsorption 2004, 20, 23.
5. Du, J.; Sun, R.; Zhang, S.; Zhang, L. F.; Xiong, C. D.; Peng, Y. X. Macromol Rapid Commun, 2004, 25, 954.
6. Du, J.; Sun, R.; Zhang, S.; Zhang, L. F.; Xiong, C. D.; Peng, Y. X. Biopolymers, 2005, 78, 1.
7. Yang, G.; Huang, Q. L.; Zhang, L. N. J Appl Polym Sci 2004, 92, 77.
8. Xiao, C. B.; Weng, L. H.; Zhang, L. N. J Appl Polym Sci 2002, 84, 2554.
9. de Carvalho, A. J. F.; Curvelo, A. A. S.; Agnelli, J. A. M. Carbohydr Polym 2001, 45, 189.
10. Park, H. M.; Li, X.; Jin, C. Z; Park, C. Y.; Chao, W. J.; Ha, C. K. Macromol Mater Eng 2002, 287, 553.
11. Park, H. M.; Liang, X. M.; Mohanty, A. K.; Misra, M.; Drazal, L. T. Macromolecules 2004, 37, 9076.
12. Zheng, J. P.; Li, P.; Ma, Y. L.; Yao, K. D. J Appl Polym Sci 2002, 86, 1189.
13. Darder, M.; Colilla, M.; Ruiz-Hitaky, E. Chem Mater 2003, 15, 3774.
14. Carrado, K. A.; Thiyagarajan, P.; Elder, D. L. Clays Clay Miner 1996, 44, 506.
15. Vaia, R. A.; Vasudevan, S.; Krawiec, W.; Scanlon, L. G.; Gianelis, E. P. Adv Mater 1995, 7, 154.
16. Jihuai, W.; Jiangming, L.; Meng, Z.; Congrong, W. Macromol Rapid Commun 2000, 21, 1032.
17. Shinsaku, K.; Shigetomo, T.; Naruhiro, H.; Yoshinori, T. Food Hydrocolloids 2002, 16, 289.
18. Strawhecker, K. E.; Manias, E. Chem Mater 2000, 12, 2943.
19. Kim, S. R.; Yuk, S. H.; Mu, S. J. Eur Polym J 1997, 33, 1009.
20. Hwan-Man, P.; Xiucuo, L.; Chang-Zhu, J.; Chan-Young, P.; Won-Jei, C.; Chang-Sik, H. Macromol Mater Eng 2002, 287, 553.
21. Jia, C.; Chen, S.; Mo, W.; Meng, Y.; Yang, L. Chin Biochem J 1988, 4, 407.
22. Xie, W.; Gao, Z. M.; Pan, W. P.; Vaia, R.; Hunter, D.; Singh, A. Polym Mater Sci Eng 2000, 82, 284.
23. Shia, D.; Hui, C. Y.; Burnside, S. D.; Giannelis, E. P. Polym Compos 1998, 19, 608.
24. Magaraphan, R.; Lilayuthalert, W.; Sirivat, A.; Schwank, J. W. Compos Sci Technol 2001, 61, 1253.
25. Pan, J. R.; Huang, C.; Chen, S.; Chung, Y. C. Colloids Surf A 1999, 147, 359.
26. Hetzel, F.; Doner, H. E. Clays Clay Miner 1993, 41, 453.